Neural Activity Reconstruction From Calcium Imaging Recordings

Yu Chen
Program in Neural Computation
Carnegie Mellon University
Pittsburgh, PA 15213
albertyuchen@cmu.edu

Aaron Rumack
Machine Learning
Carnegie Mellon University
Pittsburgh, PA 15213
arumack@andrew.cmu.edu

Darby Losey
Program in Neural Computation
Carnegie Mellon University
Pittsburgh, PA 15213
dlosey@andrew.cmu.edu

1 Introduction

Optical imaging is a relatively novel method in neuroscience that allows for many neurons to be recorded simultaneously. Neural action potentials are accompanied with a changing flow of calcium ions through the neural membrane, which induces an optically measurable response in calcium fluorescence dynamics. The signal is characterized by a transient rising phase due to the onset of action potentials, and a slowly exponentially decreasing phase after neuronal firing ceases. How to best extract the underlying neural activity given this optical signal is an open problem. Specifically, this problem is made non-trivial due to background noise, effects from adjacent neurons, and complications from the times series dynamics [17, 15]. Here we present a systematic review of existing techniques and their relationship to optimization. We expand the current state of the field by providing various new frameworks. Additionally, we implemented a subset of these frameworks and provide demonstrations of their effectiveness.

2 Related Works

2.1 Spatial-temporal deconvolution method

A recent work [17] extracts both spatial positions of neurons in the calcium recording videos, and temporal events. The algorithm iteratively optimizes over both spatial and temporal models. To be more specific, the calcium signal model is the following:

$$Y = \sum_{i=1}^{K} a_i c_i^T + B + E = AC + B + E \tag{1}$$

Where the video data is represented by a matrix $Y \in \mathbb{R}^{d \times T}$ such that each column represents a frame vectorized into a d array. The length of the recording is T frames. The i^{th} neuron is characterized by its spatial "footprint" vector $a_i \in \mathbb{R}_+^d$ depicting the neuron's shape and location. The calcium signal time series $c_i \mathbb{R}_+^T$ modeling the neurons mean fluorescence signal. The noise $E \in \mathbb{R}^{d \times T}$ is assumed as Gaussian, $E(t) \sim \mathcal{N}(0, \Sigma)$. Σ is a diagonal matrix, assuming that the noise is spatially and temporally uncorrelated. The authors characterize the fluorescence signal such that it behaves in a pattern of transient rising when there are neural activity events s_i, and exponentially decreasing

32nd Conference on Neural Information Processing Systems (NIPS 2018), Montréal, Canada.

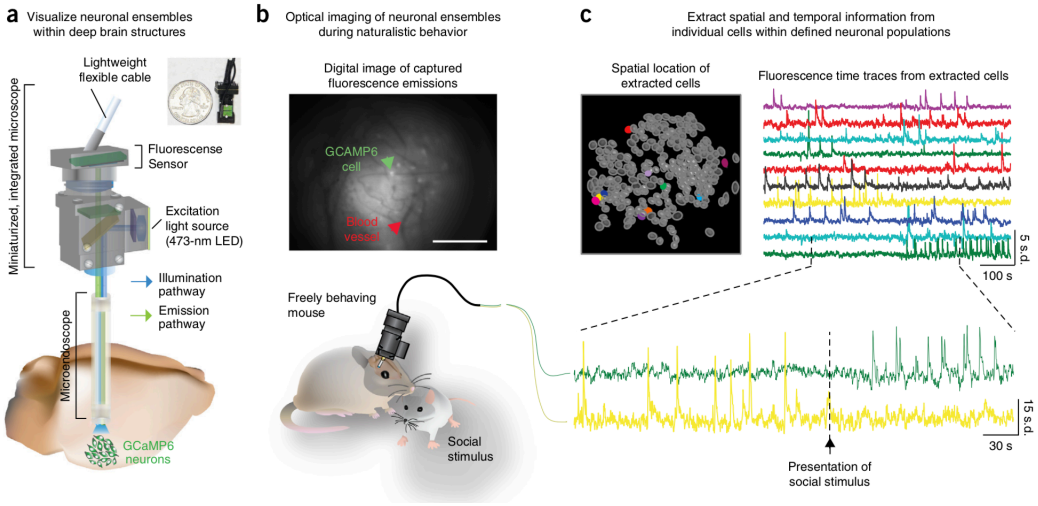

Figure 1: An example of in vivo calcium imaging recording on a rat. The recording device is in panel a. One frame of the video is in figure b. Selected neuron's spatial positions and extracted time series of the fluorescence are shown in panel c. The figure is from [11]. The sampling rate of the recording is 15 Hz, while the length of a unit action potential is around 1 ms. The goal of the deconvolution methods is to extract underlying neural activity of the recordings of visual signal.

otherwise [10, 14]. Thus the response fluorescence signal can be treated as the convolution of the event sequence and an exponential kernel,

$$c_i(t) = \sum_{j=1}^{p} \gamma_j^{(i)} c(t-j) + s_i(t) \tag{2}$$

For simplicity, we take $p = 1$. This simplification matches the real data quite well. It is worth noting that the neural activity s_i are positive values and not discrete integers or binary values. This is due to the the nonlinearity of the fluorescence response. Stated differently, the addition of action potentials do not necessarily trigger an addition increase in the fluorescence strength as the fluorescence measurements can become get saturated with strong bursts [15]. Within the time interval of calcium imaging (which has a sampling frequency of several tens of Hertz), the precise position is difficult to infer, which could also make the response nonlinear. The convolution can be expressed as $G^{(i)}c_i = s_i$ inversely, where $G^{(i)}$ is the deconvolution matrix corresponding to the exponential kernel [7, 15, 17]. One important improvement of this work is addressing the issue of background noise, both globally and locally. [17] noticed that background noise is a serious issue in signal extraction. This can significantly diminish the performance of the methods based on correlation [12]. In the preprocessing step, Zhou et al. use a mean subtracted filter to spatially smooth the video, which turned out to be very effective. The background is decomposed into $B = B^f + B^c$, $B^c = b_0\mathbf{1}^T$ is the constant offset, B^f is the fluctuating signal, where $B^f_{i,g} = \sum_{j\in\Omega_i} w_{ij} B^f_{j,g}$, $\Omega_i = \{j \mid \|x_i - x_j\|_2 \in [l_n, l_n + 1]\}$, which indicates neighboring pixels with distance l_n from the i'th pixel. In summary, the goal is to optimize the following problem,

$$\begin{aligned}
\min_{A,C,S,B^f,W,b_0} \quad & \|Y - AC - B^f - b_0\mathbf{1}^T\|_F^2 \\
\text{subject to} \quad & A \geq 0 \quad \text{element-wise, and is sparse and spatially localized} \\
& c_i, s_i \geq 0, G^{(i)}c_i = s_i, s_i \text{ is spare.} \\
& B^f\mathbf{1} = 0 \\
& B^f = W(Y - AC - b_0\mathbf{1}^T) \\
& W_{ij} = 0 \text{ if } \|x_i - x_j\|_2 \notin [l_n, l_n + 1)
\end{aligned} \tag{3}$$

The overall problem is non-convex, but it can be optimized iteratively by fitting parameters separately [17].

2.2 An fast algorithm with ℓ_0 constraint

The second representative work is done by [9, 8]. This method does not consider the spatial location of neurons in the field of view. Instead they start with the extracted fluorescence of each neuron with well performed background subtraction. Their model is,

$$y_t = \beta_0 + c_t + \epsilon_t, \quad \epsilon_t \sim \mathcal{N}(0, \sigma^2) \tag{4}$$

$$c_t = \gamma c_{t-1} + s_t, \quad t = 1, ..., T \tag{5}$$

The notations are the same as the last paragraph. In this model, the calcium fluorescence only depends on the value during the last time interval, and decreases after neural activity events, which is the same as [17]. They do not consider the fluctuating background with local information, assuming instead that it is constant. Thus, the goal is to optimize the following equation,

$$\min_{\substack{c_1,...,c_T \\ s_2,...,s_T}} \quad \left\{ \frac{1}{2} \sum_{t=1}^{T} (y_t - c_t)^2 + \lambda \sum_{t=2}^{T} I(s_t \neq 0) \right\} \tag{6}$$

$$\text{subject to} \quad s_t = c_t - \gamma c_{t-1} \geq 0 \tag{7}$$

The ℓ_0 penalty forces the solution of s_t to be sparse. It also has to be non-negative due to the biophysiological constraint that that the action potential count for each neuron is nonnegative and action potentials can only cause a positive calcium fluorescence response. [9] show that this problem can be solved efficiently by dropping the condition that $c_t - \gamma c_{t-1} \geq 0$, which is,

$$\min_{\substack{c_1,...,c_T \\ s_2,...,s_T}} \quad \left\{ \frac{1}{2} \sum_{t=1}^{T} (y_t - c_t)^2 + \lambda \sum_{t=2}^{T} I(s_t \neq 0) \right\} \tag{8}$$

$$\text{subject to} \quad s_t = c_t - \gamma c_{t-1} = 0 \tag{9}$$

In their later paper [8], the authors facilitate the algorithm to make the computation much more efficient. Additionally, as this problem is nonconvex, it can be relaxed without a substantial loss in performance:

$$\min_{\substack{c_1,...,c_T \\ s_2,...,s_T}} \quad \left\{ \frac{1}{2} \sum_{t=1}^{T} (y_t - c_t)^2 + \lambda \sum_{t=2}^{T} ||s_t|| \right\} \tag{10}$$

$$\text{subject to} \quad s_t = c_t - \gamma c_{t-1} \geq 0 \tag{11}$$

2.3 A Bayesian model

The third work given by [15] uses Bayesian inference. The calcium fluorescence response model is still the same as equation 2 [14]. Authors assume that the $s_i \sim$ Bernoulli(p), and the probability is independent of time. Stated differently, the firing rate of a neuron is homogeneous across time. In this work, authors add one more layer between calcium ion concentration and the observation of fluorescence.

$$[\text{Ca}^{2+}]_t - [\text{Ca}^{2+}]_{t-1} = -\frac{\Delta}{\tau}([\text{Ca}^{2+}]_{t-1} - [\text{Ca}^{2+}]_b) + As_t + \sigma_c \sqrt{\Delta} \epsilon_{c,t} \tag{12}$$

$$F_t = \alpha [\text{Ca}^{2+}]_t + \beta + \sigma_F \epsilon_{F,t} \tag{13}$$

σ_c scales the Gaussian noise of calcium ion concentration $\epsilon_{c,t}$. σ_F scales the fluorescence strength. In addition, they relax assumptions to incorporate nonlinear saturation of the fluorescence signal, as well as external stimulus and history dependent events, such as neural refactory periods. The

observations are $\mathbf{O}_t = F_t$. The hidden states are $\mathbf{H}_t = \{s_t, [\text{Ca}^{2+}]_t\}$. The parameters are $\boldsymbol{\theta} = \{\tau, [\text{Ca}^{2+}]_b, A, \sigma_c, \sigma_F, p\}$. The overall model is,

$$\mathbb{P}_{\boldsymbol{\theta}}(\mathbf{O}_{1:T}, \mathbf{H}_{1:T}) = \mathbb{P}_{\boldsymbol{\theta}}(\mathbf{H}_0) \prod_{t=1}^{T} \mathbb{P}_{\boldsymbol{\theta}}(\mathbf{H}_t|\mathbf{H}_{t-1}) \mathbb{P}_{\boldsymbol{\theta}}(\mathbf{O}_t|\mathbf{H}_t) \tag{14}$$

The probability of the observed fluorescence give the underlying calcium ion concentration and the neural activities,

$$\begin{aligned} \mathbb{P}_{\boldsymbol{\theta}}(\mathbf{O}_t|\mathbf{H}_t) &= \mathbb{P}_{\boldsymbol{\theta}}(F_t|[\text{Ca}^{2+}]_t, s_t) = \mathbb{P}_{\boldsymbol{\theta}}(F_t|[\text{Ca}^{2+}]_t) \\ &= \mathcal{N}(F_t; \alpha[\text{Ca}^{2+}]_t + \beta, \sigma_F^2) = \mathcal{N}(F_t; [\text{Ca}^{2+}]_t, 1) \end{aligned} \tag{15}$$

The probability of hidden states transition,

$$\begin{aligned} \mathbb{P}_{\boldsymbol{\theta}}(\mathbf{H}_t|\mathbf{H}_{t-1}) =& \mathbb{P}_{\boldsymbol{\theta}}(F_t, s_t|F_{t-1}, s_{t-1}) \\ =& \mathbb{P}_{\boldsymbol{\theta}}(F_t|F_{t-1}, s_{t-1}) \mathbb{P}_{\boldsymbol{\theta}}(s_t) \\ =& \mathcal{N}(\text{Ca}^{2+}]_t : \mu(s_t), \sigma_c^2) p^{s_t} (1-p)^{1-s_t} \\ \text{where} \quad \mu(s_t) =& [\text{Ca}^{2+}]_{t-1} - \frac{\Delta}{\tau}([\text{Ca}^{2+}]_{t-1} - [\text{Ca}^{2+}]_b) + A s_t + \sigma_c \end{aligned} \tag{16}$$

The conditional independence between the probability of fluorescence and neural activities is due the homogeneous Bernoulli assumption. The authors use a particle filter to approximate the forward recursion. The goal of the problem is to infer neural activity given the observation $\mathbb{P}_{\boldsymbol{\theta}}(\mathbf{H}_{1:T}|\mathbf{O}_{1:T})$. This inference may be well approximated by generating a number of weighted samples (i.e. "particles")[6].

2.4 Nonlinearity of the fluorescence response signal

According to both a public competition [2] scoreboard and [5], the unsupervised *MLspike* method out performs other methods, including some supervised learning method. Two potential significant advantages are their nonlinear model for the fluorescence response to the calcium concentration and fluctuating background. Their model is the following,

$$c_t = \gamma c_{t-1} + n_t \tag{17}$$

$$B_t = B_{t-1} + \eta w_t \tag{18}$$

$$F_t = B_t(1 + A\frac{c_t}{1+\nu c_t}) + \sigma\epsilon_t \tag{19}$$

Where ϵ and w_t are independent unit Gaussian random variables. Authors model the fluorescence responses in separate steps. The exponentially decreasing calcium concentration assumption is the same as previous subsections. The fluctuation background is modeled with a brownian motion. The fluorescence response is a nonlinear function of calcium concentration. If $\nu = 0$, it is equivalent to previous method. If c_t is a large value, the fluorescence will get saturated. This nonlinear effects have been reported by [3, 16, 13]. The goal of the model is to maximize the target equation below,

$$\hat{\mathbf{x}} = \arg\max_{\mathbf{x}} p(\mathbf{x}|\mathbf{F}) \tag{20}$$

$\mathbf{x} = \{(n_i, B_1), ..., (n_T, B_T)\}$ contains the hidden variables. $\mathbf{F}$ is the observed fluorescence signal. The above equation can be decomposed into the following akin to hidden Markov chain,

$$p(\mathbf{x}|\mathbf{F}) = p(x_1)p(F_1|x_1)p(x_2|x_1)p(F_2|x_2)...p(x_T|x_{T_1})p(F_T|x_T) \tag{21}$$

The expansion is based on assuming $x_{t+1}, ..., x_T, F_{t+1}, ..., F_T$ are independent of $F_t, x_{t-1}, F_{t-1}, ..., x_1, F_1$ given x_t. As for the hidden states transition probability and conditional observation probability,

$$p(x_t|x_{t-1}) = \lambda^k \frac{e^{-k\lambda}}{k!}, \quad \text{if } \exists k, \text{s.t. } c_t - \gamma c_{t-1} + k \tag{22}$$

$$p(F_t|x_t) = N\left(B_t(1 + A\frac{c_t}{1+\nu c_t}), \sigma^2\right) \tag{23}$$

3 Methods

3.1 Trend filtering for background denoising

OASIS is a state-of-the-art method for detecting neural activity [7]. The heart of OASIS utilizes interior point methods to solve the following convex optimization problem:

$$\begin{aligned} \min_{\mathbf{c},\mathbf{s}} \ & \|\mathbf{y}-\mathbf{c}\|^2 + \lambda_s \|\mathbf{s}\|_1 \\ \text{subject to } \ & \mathbf{s} = G\mathbf{c} \\ & \mathbf{s} \geq 0 \end{aligned} \tag{24}$$

where $\mathbf{y}$ is the observed fluorescence, $\mathbf{c}$ and $\mathbf{s}$ are the estimated fluorescence and spikes respectively. G denotes the convolution matrix, specifically:

$$G = \begin{bmatrix} 1 & 0 & 0 & ... \\ -\gamma & 1 & 0 & ... \\ 0 & -\gamma & 1 & ... \\ ... & & & \end{bmatrix}$$

We re-implemented this component of OASIS in order to identify and investigate any prevalent systematic errors. Specifically, we found that, in many instances, it does not properly capture the rate of decay in the fluorescence. We hypothesized that this is due to the model not properly accounting for noise in the baseline fluorescence. Thus we formulated the following convex model:

$$\begin{aligned} \min_{\mathbf{c},\mathbf{s},\mathbf{b},\mathbf{u}} \ & \|\mathbf{y}-\mathbf{c}-\mathbf{b}\|^2 + \lambda_u \|\mathbf{u}\|_1 + \lambda_b \|\mathbf{b}\|_2 + \lambda_s \|\mathbf{s}\|_1 \\ & \text{subject to } \ \mathbf{s} = G\mathbf{c} \\ & \mathbf{u} = D\mathbf{b} \\ & \mathbf{s} \geq 0 \end{aligned} \tag{25}$$

where $\mathbf{b}$ is the estimated background noise. We choose to use second order trend filtering. In practice, in order to let the filter to better constrain the whole timecourse smoothness, we shift the off-diagonal by 2 steps, so that the second derivative is calculate using data points little further away.

$$D = \begin{bmatrix} -2 & 0 & 0 & 1 & ... & & & \\ 0 & -2 & 0 & 0 & 1 & ... & & \\ 0 & 0 & -2 & 0 & 0 & 1 & ... & \\ 1 & 0 & 0 & -2 & 0 & 0 & 1 & ... \\ & & ... & & & & & \end{bmatrix} \tag{26}$$

Using trend filtering helps insure the background noise is smooth across time, while the L2 penalty on the background noise helps avoid over-fitting. Deconvolving the calcium trace provides a windowed spiking estimate. Since the absolute time of spike firing is a non-identifiable problem, we illustrate our results using cross-correlation against the true poststimulus time histogram.

3.2 Sparser reconstruction using L0 penalty

Because the L1 penalized problem produces solutions that are not sparse enough, [9] use an L0 penalty to obtain a better solution. Although this makes the problem nonconvex, the authors design an algorithm to solve the problem in polynomial time. They solve the problem

$$\begin{aligned} \min_{\mathbf{c},\mathbf{s}} \ & \|\mathbf{y}-\mathbf{c}\|^2 + \lambda_s \|\mathbf{s}\|_0 \\ \text{subject to } \ & \mathbf{s} = G\mathbf{c} \\ & \mathbf{s} \geq 0 \end{aligned} \tag{27}$$

where $\mathbf{y}$, $\mathbf{c}$, $\mathbf{s}$ and G are the observed fluorescence, estimated fluorescence, spike train, and convolution matrix as above. The authors reduce this problem to a changepoint detection problem:

$$\min_{0=\tau_0<\tau_1<\cdots<\tau_k<\tau_{k+1}=T,k} \left\{ \sum_{j=0}^{k} \mathcal{D}(y_{(\tau_j+1):\tau_{j+1}}) + \lambda k \right\} \\ \text{where } \mathcal{D}(y_{a:b}) = \min_{\alpha} \left\{ \frac{1}{2} \sum_{t=a}^{b} (y_t - \alpha\gamma^{t-b})^2 \right\} \tag{28}$$

$\mathcal{D}$ represents the distance between the observed and estimated fluorescence signal between each pair of spikes. This can be solved using dynamic programming in $O(T^2)$ time, where T is the number of time points. [8] make the computation even more efficient, so that solving the problem for $T = 100000$ takes less than a second.
Both the L1-penalized problem and the L0-penalized problem do not produce sparse enough outputs, and predict spikes that are too close together to be biologically feasible. Therefore, we further modify our approach.

3.3 Bayesian reconstruction

We notice that in the binned spike train with bin width of 10ms, most bins contain either 0 spikes or 1 spike. Only a few bins have 2, and they rarely have 3 spikes or more. This is biophysiologically reasonable due to the refractory period, which is around 3-4 ms [1]. When the neuron has higher firing rate, the output using L1 penalty cannot have output sparse enough. This motivates us to use integers in range $\{0, 1, 2, 3\}$ to make the results more sparse, and get biologically realistic action potentials. However, in general, integer programming is not a strict convex optimization problem, and an exact solution is an NP problem [4]. Some approximate solutions usually requires a simple form of the problem, which can not be easily adapted to the problem in equation 25. For the calcium imaging and spike train time sequences, events have temporal dependence, such as the exponential decay of the fluorescence signal, and the sharp increases trigger by action potentials. Thus, we treat the fluorescence signals and underlying spike trains as a hidden Markov chain, where the spike trains contribute to the hidden states, and the noisy observed signal depends on the model fluorescence signal. The transition between model fluorescence signal follows the rule of exponential decay. The goal is to find the most likely spike trains matching the observed signal. In these method, we use the background corrected signal as the input.

$$\begin{aligned} &\max_{\mathbf{n},\boldsymbol{\theta}} \; p(\mathbf{c}|\mathbf{y};\boldsymbol{\theta}) = \max_{\mathbf{n},\boldsymbol{\theta}} \; p(\mathbf{y}|\mathbf{c})p(\mathbf{c}) \\ =&\max_{\mathbf{n},\boldsymbol{\theta}} \; p(c_0) \prod_{t=2}^{T} p(c_t|c_{t-1}) \prod_{t=1}^{T} p(y_t|c_t) \end{aligned} \tag{29}$$

y_t is the observed fluorescence signal, c_t is the model signal.

$$p(y_t|c_t) = \frac{1}{\sqrt{2\pi}\sigma} \exp\{-\frac{1}{2\sigma^2}(y_t - c_t)^2\} \tag{30}$$

$$p(c_t|c_{t-1}) = \begin{cases} e^{\lambda} \frac{\lambda^k}{k!} & \text{if } |c_t - \gamma c_{t-1} - An_k| \le \tau_c, \qquad k \in \{0, 1, 2, 3\} \\ 0 & \text{otherwise} \end{cases} \tag{31}$$

The most likely sequence can be estimated backward along the Markov chain, similar to Viterbi's algorithm.

$$\begin{aligned} M(c_t, t) =& \max_{\mathbf{n}_{t+1:T}} p(\mathbf{c}_{t+1:T}, \mathbf{y}_{t:T}|c_t) \\ =& p(y_t|c_t) \max_{\mathbf{n}_{t+1:T}} p(c_{t+1}|c_t) p(\mathbf{c}_{t+2:T}, \mathbf{y}_{t+1:T}|c_{t+1}) \\ \approx& p(y_t|c_t) \max_{n_{t+1}} p(c_{t+1}|c_t) M(c_{t+1}, t+1) \end{aligned} \tag{32}$$

The c_t and n_t can be obtained by calculating $M(c_t, t)$ from T to 1. We follow the method in [7, 5] to tune the parameter σ, τ_c, γ.

4 Results

With correction of background, we achieve higher performance in neural activity reconstruction. The slow changing background is usually unobserved, and this can lead to both false positive and false negative. For example, when the background is increasing, the model without consideration of this artifact will output more spikes. When the background is decreasing, it will detect less spikes vice verse. We notice that the background changes much slower compared to the transient changes triggered by action potentials, so without the correction of the background, it will result in obvious systematical error, usually comes with more false positives cases than false negative cases in a large range, and the other way in some other ranges.

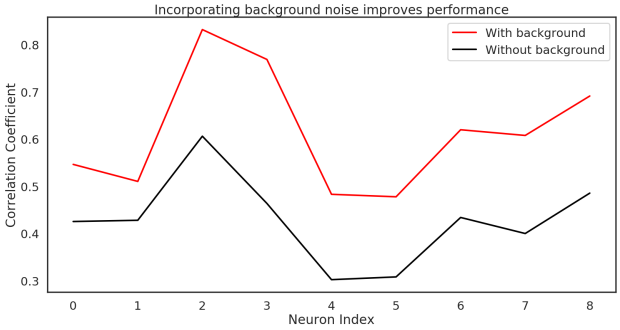

Figure 2: Our method outperforms the core OASIS method for 9 tested datasets.

By using the background corrected florescence signal, we further parse the neural activities into a sequence of integer, which is more biophysiologically realistic. By inheriting the advantages of the background correction method, the predicted fluorescence signal reconstructed by Bayesian method matches the real signal quite well as shown in figure 3. With contaminated noise, exact timestamps are hard to be recovered, but the smoothed neural activities matches the real recordings quite well (data not shown).

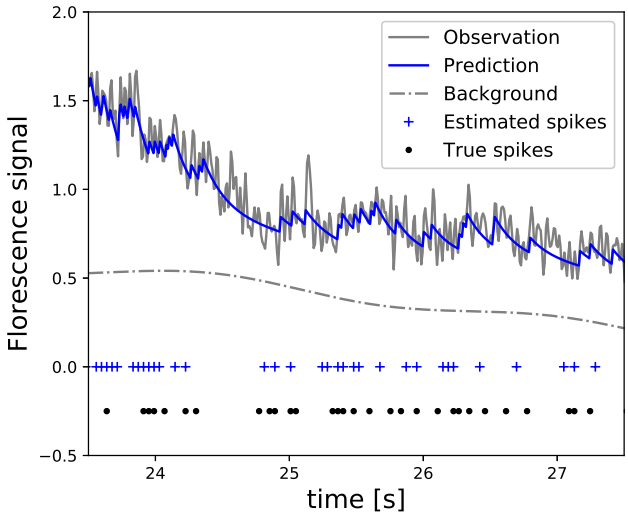

Figure 3: Reconstructed fluorescence signal, neural activities and background.

5 Conclusions and Future Plan

We provide several novel methods of estimating neural activity from fluorescence signals, show the experimental results from two of these frameworks and provide evidence that one of these methods is an improvement upon a state-of-the-art algorithm. We reviewed several existing calcium imaging methods and detailed their relationship to the convex optimization methods detailed in class. We intend to continue work on this project in hopes of eventual publication. Specifically, we intend to:

- Estimate the background fluorescence with a Gaussian process
- Refine the Bayesian method using a backward-forward method, and increase the order of Markov chain
- Optimize our algorithms and formulate our code into a publicly available package

References

[1] Refractory period. `http://www.physiologyweb.com/lecture_notes/neuronal_action_potential/neuronal_action_potential_refractory_periods.html`. Accessed: 2019-12-12.

[2] Spike finder. `http://spikefinder.codeneuro.org`. Accessed: 2018-11-17.

[3] Jasper Akerboom, Tsai-Wen Chen, Trevor J Wardill, Lin Tian, Jonathan S Marvin, Sevinç Mutlu, Nicole Carreras Calderón, Federico Esposti, Bart G Borghuis, Xiaonan Richard Sun, et al. Optimization of a gcamp calcium indicator for neural activity imaging. *Journal of Neuroscience*, 32(40):13819–13840, 2012.

[4] Michele Conforti, Gérard Cornuéjols, and Giacomo Zambelli. Integer programming models. In *Integer Programming*, pages 45–84. Springer, 2014.

[5] Thomas Deneux, Attila Kaszas, Gergely Szalay, Gergely Katona, Tamás Lakner, Amiram Grinvald, Balázs Rózsa, and Ivo Vanzetta. Accurate spike estimation from noisy calcium signals for ultrafast three-dimensional imaging of large neuronal populations in vivo. *Nature communications*, 7:12190, 2016.

[6] Arnaud Doucet, Nando De Freitas, and Neil Gordon. An introduction to sequential monte carlo methods. In *Sequential Monte Carlo methods in practice*, pages 3–14. Springer, 2001.

[7] Johannes Friedrich, Pengcheng Zhou, and Liam Paninski. Fast online deconvolution of calcium imaging data. *PLoS computational biology*, 13(3):e1005423, 2017.

[8] Sean Jewell, Toby Dylan Hocking, Paul Fearnhead, and Daniela Witten. Fast nonconvex deconvolution of calcium imaging data. *arXiv preprint arXiv:1802.07380*, 2018.

[9] Sean Jewell and Daniela Witten. Exact spike train inference via l_0 optimization. *arXiv preprint arXiv:1703.08644*, 2017.

[10] Eftychios A Pnevmatikakis, Daniel Soudry, Yuanjun Gao, Timothy A Machado, Josh Merel, David Pfau, Thomas Reardon, Yu Mu, Clay Lacefield, Weijian Yang, et al. Simultaneous denoising, deconvolution, and demixing of calcium imaging data. *Neuron*, 89(2):285–299, 2016.

[11] Shanna L Resendez, Josh H Jennings, Randall L Ung, Vijay Mohan K Namboodiri, Zhe Charles Zhou, James M Otis, Hiroshi Nomura, Jenna A McHenry, Oksana Kosyk, and Garret D Stuber. Visualization of cortical, subcortical and deep brain neural circuit dynamics during naturalistic mammalian behavior with head-mounted microscopes and chronically implanted lenses. *Nature protocols*, 11(3):566, 2016.

[12] Spencer L Smith and Michael Häusser. Parallel processing of visual space by neighboring neurons in mouse visual cortex. *Nature neuroscience*, 13(9):1144, 2010.

[13] Lai Hock Tay, Oliver Griesbeck, and David T Yue. Live-cell transforms between ca2+ transients and fret responses for a troponin-c-based ca2+ sensor. *Biophysical journal*, 93(11):4031–4040, 2007.

[14] Joshua T Vogelstein, Adam M Packer, Timothy A Machado, Tanya Sippy, Baktash Babadi, Rafael Yuste, and Liam Paninski. Fast nonnegative deconvolution for spike train inference from population calcium imaging. *Journal of neurophysiology*, 104(6):3691–3704, 2010.

[15] Joshua T Vogelstein, Brendon O Watson, Adam M Packer, Rafael Yuste, Bruno Jedynak, and Liam Paninski. Spike inference from calcium imaging using sequential monte carlo methods. *Biophysical journal*, 97(2):636–655, 2009.

[16] Ryohei Yasuda, Esther A Nimchinsky, Volker Scheuss, Thomas A Pologruto, Thomas G Oertner, Bernardo L Sabatini, and Karel Svoboda. Imaging calcium concentration dynamics in small neuronal compartments. *Sci. STKE*, 2004(219):pl5–pl5, 2004.

[17] Pengcheng Zhou, Shanna L Resendez, Jose Rodriguez-Romaguera, Jessica C Jimenez, Shay Q Neufeld, Andrea Giovannucci, Johannes Friedrich, Eftychios A Pnevmatikakis, Garret D Stuber, Rene Hen, et al. Efficient and accurate extraction of in vivo calcium signals from microendoscopic video data. *ELife*, 7:e28728, 2018.